

Intermolecular Dynamical Charge Fluctuations in Water: A Signature of the H-Bond Network

Manu Sharma,¹ Raffaele Resta,^{2,3} and Roberto Car¹

¹*Department of Chemistry and Princeton Institute for the Science and Technology of Materials, Princeton University, Princeton, New Jersey 08544, USA*

²*INFN DEMOCRITOS National Simulation Center, via Beirut 2, I-34014 Trieste, Italy*

³*Dipartimento di Fisica Teorica, Università di Trieste, Strada Costiera 11, I-34014 Trieste, Italy*
(Received 29 October 2004; revised manuscript received 15 April 2005; published 25 October 2005)

We report a simulation of deuterated water using a Car-Parrinello approach based on maximally localized Wannier functions. This provides local information on the dynamics of the hydrogen-bond network and on the origin of the low-frequency infrared activity. The oscillator strength of the translational modes, peaked around $\sim 200\text{ cm}^{-1}$, is anisotropic and originates from intermolecular—not intramolecular—charge fluctuations. These fluctuations are a signature of a tetrahedral hydrogen-bonding environment.

DOI: [10.1103/PhysRevLett.95.187401](https://doi.org/10.1103/PhysRevLett.95.187401)

PACS numbers: 78.30.Cp, 32.10.Dk, 61.25.Em, 71.15.Pd

Water is an unusual liquid due to the network of highly directional H bonds that connect adjacent molecules. The crucial role that water plays in chemistry and biology is largely a consequence of its H-bond network [1]. The dynamics of this network has signatures in the far infrared (IR) spectrum [2,3]. This exhibits a prominent peak at $\sim 200\text{ cm}^{-1}$ [4], which is the main topic of the present investigation. A feature at $\sim 60\text{ cm}^{-1}$ has sometimes been discussed, but its infrared signature is very weak and is only detected below room temperature [5]. The feature at $\sim 200\text{ cm}^{-1}$ is associated to hindered translational motions of the water molecules [3]. Since translations of rigid (nonpolarizable) neutral molecules do *not* couple to electromagnetic fields, classical simulations [6–8] have addressed the IR activity of the translational modes by means of force fields, where each molecule is polarized according to the local field: the induced polarization is thus *intramolecular*. Here we adopt a first-principles approach, where the liquid is regarded as an assembly of electrons and nuclei. We find that polarization effects depend on the environment in a strong *intermolecular* way.

We report a calculation of the IR spectrum of liquid water using a modified Car-Parrinello (CP) approach [9,10], in which maximally localized Wannier functions (MLWFs) [11] are used in place of delocalized Bloch orbitals to represent “on the fly” the electronic wave functions. Our simulation [12] produces a spectrum in good agreement with experiment. MLWFs show that only the hindered translational modes associated to asymmetric changes in the H-bond environment of a tagged molecule are IR active.

We consider here deuterated water D_2O , which in experiments exhibits a low-frequency peak at $\sim 185\text{ cm}^{-1}$ [2]. Given that the onset of intramolecular bond-bending and bond-stretching modes in D_2O is above 1200 cm^{-1} , the mechanisms responsible for the low-frequency peak can be understood in a picture in which the molecular frames are essentially rigid.

Within classical simulations each molecule in the fluid is a well-defined entity, carrying a permanent and a dynamic induced dipole, the latter depending on the environment only via the value of the local field at the molecular center. By contrast, in a quantum-mechanical picture the electron distribution in the fluid *cannot* be partitioned into terms unambiguously attributed to individual molecules. In a quantum picture the electron distribution around the nuclear frame of each molecule is strongly affected by its environment.

H bonds are responsible for the local tetrahedral coordination of the O atoms, and for the Pauling ice-rule geometry of the H atoms. In the liquid, not all the molecules are tetrahedrally coordinated and H bonds continuously break and reform. In our simulation we consider a molecule to be tetrahedrally coordinated if it has four oxygen nearest neighbors and these belong to four non-face-sharing octants associated to a Cartesian frame centered on the oxygen atom of the tagged molecule. These tetrahedral configurations have a typical lifetime of $\approx 0.2\text{ ps}$, while individual H bonds exist on average for $\approx 0.8\text{ ps}$ [18]. A typical tetrahedral configuration from a snapshot of the simulation is shown in Fig. 1(a).

While in a classical simulation the dipole of each molecule is well defined at any time, in a quantum-mechanical simulation, owing to the delocalized nature of the electron distribution, the molecular dipoles are ill defined [19]. However, *variations* $\Delta\mathbf{P}$ of the macroscopic polarization of a condensed sample are well defined and measurable, at least via “gedanken” experiments [20,21]. $\Delta\mathbf{P}$ for the translational modes has been expressed in Ref. [19] in terms of a dynamical molecular charge tensor $Z_{\alpha\beta}$ (Greek subscripts denote Cartesian components) which measures the polarization change induced by rigid translations of a tagged molecule in a sample of volume Ω . The dynamical molecular charge tensor generalizes the well-known concept of effective charge tensor in polar crystals [21,22]. To linear order in the molecular displacement \mathbf{u}

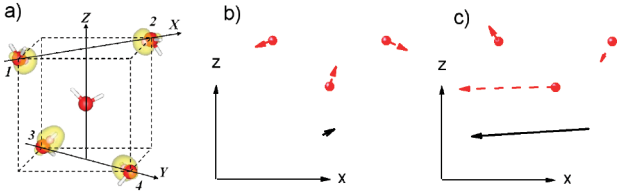


FIG. 1 (color). (a) Instantaneous tetrahedral environment of a molecule. The O neighbors are labeled 1 to 4; the x axis connects 1 and 2; the y axis connects 3 and 4; the z axis connects the center of 1–2 with the center of 3–4. This local frame is not orthogonal but the deviation is usually small. 1, 2, 3, and 4 identify a “cubic” cage shown by dashed lines, the center of which is near the O of the central molecule. The isodensity plots show MLWFs of the corner molecules participating in H bonds with the central molecule. The 1 and 2 MLWFs are lone pairs; 3 and 4 are bond pairs. The central molecule forms donor bonds with 1 and 2 and acceptor bonds with 3 and 4 (Pauling ice rule). In (b) and (c) the red dashed arrows show molecular dipole changes induced by a displacement of the central molecule along z (b) and $-x$ (c); the full black arrows show the net effect of the coordinated dipolar changes.

the polarization change is $\Delta P_\alpha = Z_{\alpha\beta} \mu_\beta / \Omega$. To eliminate the dependence of $\Delta \mathbf{P}$ from the shape of the sample it is customary to specify the macroscopic field \mathbf{E} in the bulk of the sample [\mathbf{E} is the *screened* field, also called “Maxwell field” [23]]. Here we follow the most common choice, which is to keep \mathbf{E} vanishing [20–22]: the same choice was also made in Ref. [19], where $Z_{\alpha\beta}$, called “dynamic molecular monopole,” was calculated as a linear-response property of the electron distribution corresponding to a liquid snapshot. The actual frequency of the modes was absent in this analysis. According to Ref. [19], the molecular charge tensor is strongly anisotropic. With reference to Fig. 1(a) the polarization change is sizeable when the central molecule is translated in the x or the y direction, whereas for translations along z the polarization change is negligible. These findings suggest that intermolecular dynamic charge fluctuations are at the origin of the polarization change. Classical models, based on point-dipole intramolecular polarizability, usually do not capture environmental effects of this kind. Indeed Madden and Impey [6] find different oscillator-strength selection rules than in Ref. [19].

Previous work showed that CP simulations, which treat quantum mechanically the electron distribution, reproduce the main experimental features of the IR spectrum, including the low-frequency peaks [24]. In our simulation four doubly occupied valence MLWFs are associated to each molecule, thus defining a neutral instantaneous charge distribution. We indicate the nuclear coordinates of the i th molecule by \mathbf{R}_O , \mathbf{R}_{D_1} , \mathbf{R}_{D_2} , respectively, and the corresponding Wannier centers by \mathbf{R}_{W_s} , $s = 1, 4$. Two MLWFs are centered on the O-D bonds and the other two are lone pairs centered on the remaining (approximately) tetrahedral directions. An instantaneous *static* molecular dipole $\boldsymbol{\mu}_i$ (in atomic units) can be defined as in

Ref. [25]:

$$\boldsymbol{\mu}_i = \mathbf{R}_{D_1} + \mathbf{R}_{D_2} + 6\mathbf{R}_O - 2 \sum_{s=1}^4 \mathbf{R}_{W_s}. \quad (1)$$

These “static” dipoles are not related to measurable properties, but their *time derivatives* or, equivalently, their *time-correlation functions*, correspond to measurable properties. The origin of the $Z_{\alpha\beta}$ tensor is in the fact that the MLWF centers do not follow rigidly the motion of the molecular frame. Instead, when neighboring molecules are displaced relative to each other, the MLWF centers move in a concerted way, and the sum of their dipoles changes by a nonzero amount. This is illustrated in Figs. 1(b) and 1(c). In Fig. 1(b) the nuclear frame of the central molecule is rigidly displaced by 0.1 Å in the z direction while all the other nuclei in the cell are fixed. The dashed red arrows show the molecular dipole changes after electronic minimization. These changes are almost entirely due to displacements of the MLWF centers associated to the lone pairs of the central molecule and to the lone pairs of molecules 1 and 2 in Fig. 1(a). Lone pairs 1 and 2 move in a manner *anticorrelated* to the lone pairs of the primary molecule, in spite of the fact that their nuclear frames are at rest. The net dipole is indicated by the black arrow and is quite small. In Fig. 1(c) we report a similar plot obtained for a displacement of the central molecule along $-x$. Here the cooperative effect is *constructive* and the net dipole is larger than the changes of the individual dipoles. The buildup of a dipole while displacing a neutral molecule effectively corresponds to a charge flow signaling an intermolecular charge transfer. We have checked that this picture is quite universal by repeating the calculation for other local tetrahedral configurations. In the liquid all the molecules move simultaneously and the actual displacements are significantly more complex than in Figs. 1(b) and 1(c). We expect that the charge transfer effect should be even enhanced in this case, because cooperative H-bond motions would extend to entire tetrahedral fluctuations.

The IR absorption coefficient is related to the power spectrum of the autocorrelation function of the macroscopic polarization \mathbf{P} [7,24]. \mathbf{P} is equal to the sum of the $\boldsymbol{\mu}_i$ in the simulation cell, divided by the cell volume [20,26]. The absorption coefficient per unit path length of a sample of volume V is:

$$\alpha(\omega) \propto \frac{\omega \tanh(\beta\hbar\omega/2)}{n(\omega)V} \int_{-\infty}^{\infty} dt e^{-i\omega t} \left\langle \sum_{ij} \boldsymbol{\mu}_i(t) \cdot \boldsymbol{\mu}_j(0) \right\rangle, \quad (2)$$

where $n(\omega)$ is the refractive index and $\beta = (k_B T)^{-1}$ is the inverse temperature [27]. Our calculated spectrum, shown in Fig. 2 [28], is in good agreement with the experimental features indicated by the arrows [2], and with the experimental relative peak intensities shown in the inset.

The largest frequency deviation from experiment occurs for the intramolecular bond-stretching modes, which have

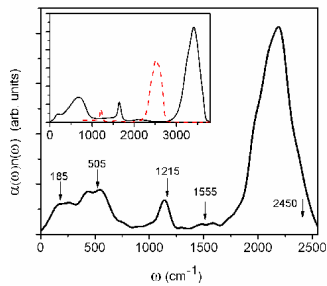


FIG. 2 (color online). Calculated D_2O IR spectrum. Arrows indicate the experimental peak positions from Ref. [2]. The full spectrum of *undeuterated* H_2O (solid line) from Ref. [4] and a spectrum of D_2O (dashed line) in the range 1000 cm^{-1} to 2800 cm^{-1} from Ref. [34] are shown in the inset.

a frequency (2200 cm^{-1}) lower than experiment by about 10%. About a third of this error is consequence of the finite fictitious electronic mass that we use in CP dynamics. The remaining error should be attributed to the finite basis set and to the approximation adopted for the exchange-correlation functional [12,14].

Besides providing the integrated quantities in Eq. (2), the MLWFs carry local information that can be used to construct “partial” correlation functions to analyze the far IR spectrum. In these calculations (reported in Figs. 3 and 5) we consider only tetrahedrally coordinated molecules; i.e., we include only the segments of trajectories in which a given molecule remains “tetrahedrally” bonded to the same four O atoms [Fig. 1(a)].

We begin with a correlation function that is purely kinematic, disregarding oscillator-strength issues. This is constructed by computing the time autocorrelation function of each of the three Cartesian displacements of an O atom with respect to the center of its associated tetrahedral cage [Fig. 1(a)]. These correlations select translational modes. The corresponding spectra, shown in Fig. 3, are strongly peaked at $\sim 200\text{ cm}^{-1}$ [29]. The figure also shows that the modes in the three Cartesian directions are equally likely. However, as we will show below, not all the three modes are IR active.

We now exploit the MLWFs to monitor the IR activity of the modes identified in the kinematic analysis. A first, very informative, experiment consists in suppressing the off-

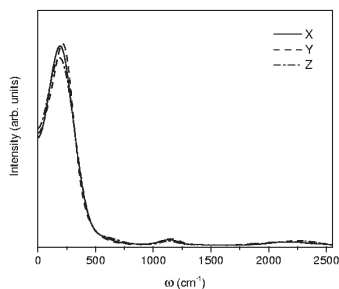


FIG. 3. Kinematical correlation function that blows up the translational modes (see text).

diagonal terms ($i \neq j$) in the double sum in Eq. (2). The resulting power spectrum, shown in Fig. 4, has no signature of the translational modes, thus perspicuously confirming our main message: the IR oscillator strength is mostly due to intermolecular charge transfer, not to dynamical fluctuations of the intramolecular dipole.

In fact, while the former comes from $i \neq j$ terms, the latter would show up even suppressing the $i \neq j$ terms. Interestingly, the molecular center-of-mass velocity autocorrelation function, also reported in Fig. 4 (dash-dotted line), shows a clear feature at $\sim 200\text{ cm}^{-1}$ in addition to a prominent peak at $\sim 60\text{ cm}^{-1}$.

We then compute the time autocorrelation function of the displacement of the centers of the four MLWFs H bonded to a tagged molecule with respect to the center of mass of this molecule, projected over the instantaneous Cartesian axes [Fig. 1(a)]. The corresponding spectra, plotted in Fig. 5, show that only the modes on the xy plane, perpendicular to the z axis of the central molecule, have a prominent peak around 200 cm^{-1} .

This is at variance with the spectrum reported in the classical simulation of Ref. [6], where the IR activity originates from dynamic dipoles induced by the local field at the molecular centers. In this approach the environment enters solely through long range Coulomb interactions. This produces an intramolecular polarization, which is strong in the molecular xz plane and weak along y . Our results indicate that the effect of the environment is more complex and due primarily to short range effects associated to concerted tetrahedral fluctuations of the H bonds [30].

Finally, we comment on the 60 cm^{-1} modes. We find, in agreement with Ref. [24], that these modes do not show IR activity. Nonetheless, they are prominent in the center-of-mass velocity autocorrelation function reported in Fig. 4. These modes correspond to H-bond *bending*, which, at variance with H-bond stretching, give rise to negligible intermolecular charge transfer. If induced intramolecular dipoles were important, they would contribute to both the 200 cm^{-1} and 60 cm^{-1} modes, as found indeed in the classical simulations of Ref. [6].

In conclusion, we have analyzed the far IR spectrum of water. We find that the translational peak at 200 cm^{-1}

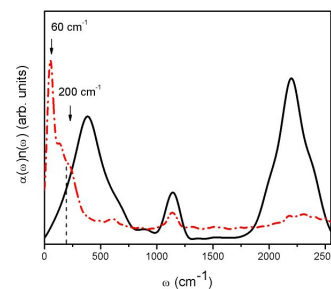


FIG. 4 (color online). IR spectrum calculated by retaining only the $i = j$ terms in the sum (solid line). Center-of-mass velocity autocorrelation function (dash-dotted line). The vertical dashed line is at 200 cm^{-1} .

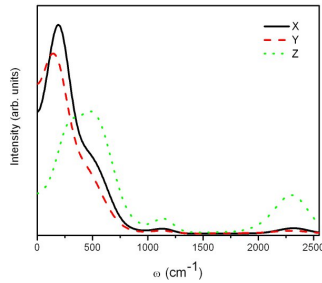


FIG. 5 (color online). Dynamical correlation functions, enhancing the IR activity due to intermolecular charge transfer (see text).

arises from intermolecular charge fluctuations associated to the H bonds of a local tetrahedral environment. Interestingly, a similar feature is present in the far IR spectrum of ice [2,31]. In supercritical water instead, where the environment is no longer tetrahedral, the vibrational feature at 200 cm^{-1} disappears [32]. The physical mechanism to which we attribute the IR feature at 200 cm^{-1} is completely different from the fluctuating intramolecular dipoles, to which this feature has been attributed so far. Intermolecular dipoles have different selection rules for IR coupling than intramolecular dipoles, suggesting that, in principle at least, the issue on the origin of the far IR feature could be settled experimentally [33].

Work was partially supported by the ONR through Grants No. N00014-01-1061, No. N00014-01-1047, and No. N00014-03-0570, and by the NSF through Grant No. CHE-0121432.

-
- [1] L. Pauling, *General Chemistry* (Freeman, San Francisco, 1970), 3rd ed. (republished by Dover, New York, 1988).
 - [2] D.S. Eisenberg and W. Kauzmann, *The Structure and Properties of Water* (Clarendon, Oxford, 1969).
 - [3] G.E. Walrafen, in *Water: A Comprehensive Treatise*, edited by F. Franks (Plenum, New York, 1972), Vol. 1, p. 151.
 - [4] J.E. Bertie and Z. Lan, *Appl. Spectrosc.* **50**, 1047 (1996).
 - [5] J.B. Hasted, S.K. Husain, F.A.M. Frescura, and J.R. Birch, *Chem. Phys. Lett.* **118**, 622 (1985).
 - [6] P.A. Madden and R.W. Impey, *Chem. Phys. Lett.* **123**, 502 (1986).
 - [7] B. Guillot, *J. Chem. Phys.* **95**, 1543 (1991).
 - [8] M. Souaille and J.C. Smith, *Mol. Phys.* **87**, 1333 (1996).
 - [9] R. Car and M. Parrinello, *Phys. Rev. Lett.* **55**, 2471 (1985).
 - [10] M. Sharma, Y. Wu, and R. Car, *Int. J. Quantum Chem.* **95**, 821 (2003).
 - [11] N. Marzari and D. Vanderbilt, *Phys. Rev. B* **56**, 12847 (1997).
 - [12] We use a periodically repeated cubic cell with 64 D_2O molecules at $T = 330\text{ K}$ and at the density of 1 g/cc in the microcanonical ensemble. We adopt norm-conserving pseudopotentials [13], a plane-wave cutoff of 60 Ry, and

the PBE XC functional [14]. The time step is 7 a.u. and the fictitious electron mass is 350 a.u. This choice gives a good description of the structure and dynamics of the liquid [15–17], with good diffusive behavior over 2 ps equilibration plus 16 ps run time.

- [13] N. Troullier and J.L. Martins, *Phys. Rev. B* **43**, 1993 (1991).
- [14] J.P. Perdew, K. Burke, and M. Ernzerhof, *Phys. Rev. Lett.* **77**, 3865 (1996).
- [15] P.L. Silvestrelli and M. Parrinello, *J. Chem. Phys.* **111**, 3572 (1999).
- [16] J.C. Grossman *et al.*, *J. Chem. Phys.* **120**, 300 (2004).
- [17] M. Allesch, E. Schwegler, F. Gygi, and G. Galli, *J. Chem. Phys.* **120**, 5192 (2004).
- [18] We define a H bond to be characterized by a O-O distance within the first minimum of $g(r)$ (3.3 \AA), and an O-D-O angle greater than 130° .
- [19] A. Pasquarello and R. Resta, *Phys. Rev. B* **68**, 174302 (2003).
- [20] R. Resta, *Rev. Mod. Phys.* **66**, 899 (1994).
- [21] W.A. Harrison, *Electronic Structure and the Properties of Solids* (Freeman, San Francisco, 1980), Sec. 5-B.
- [22] Ph. Ghosez, J.-P. Michenaud, and X. Gonze, *Phys. Rev. B* **58**, 6224 (1998).
- [23] P. Madden and D. Kivelson, *Adv. Chem. Phys.* **56**, 467 (1984).
- [24] P.L. Silvestrelli, M. Bernasconi, and M. Parrinello, *Chem. Phys. Lett.* **277**, 478 (1997).
- [25] P.L. Silvestrelli and M. Parrinello, *Phys. Rev. Lett.* **82**, 3308 (1999).
- [26] R.D. King-Smith and D. Vanderbilt, *Phys. Rev. B* **47**, R1651 (1993).
- [27] D.A. McQuarrie, *Statistical Mechanics* (University Science Books, Sausalito, California, 2000).
- [28] In the spectra of Figs. 2 and 4 we use a Fourier filter to eliminate fluctuations with a width smaller than $\sim 50\text{ cm}^{-1}$. No filter is used in the spectra of Figs. 3 and 5, which are calculated on shorter trajectories.
- [29] Configurations in which at least one of the H bonds is broken are short lived (less than 0.1 ps) and do not contribute an identifiable peak at 200 cm^{-1} .
- [30] A similar effect is allowed in the popular shell model for ionic crystals when the displacement of the electronic shell of a given ion is hindered by its first neighbors. See, e.g., A.A. Maradudin, E.W. Montroll, G.H. Weiss, and I.P. Ipatova, *Theory of Lattice Dynamics in the Harmonic Approximation*, Solid State Physics, Suppl. Vol. 3 (Academic, New York, 1971).
- [31] J.E. Bertie and E. Whalley, *J. Chem. Phys.* **40**, 1637 (1964).
- [32] G.E. Walrafen, Y.C. Chu, and G.J. Piermarini, *J. Phys. Chem.* **100**, 10363 (1996).
- [33] In a hypothetical experiment one could preferentially orient the water molecules by means of an intense dc field, and study the IR response to a radiation field while varying the direction of its linear polarization.
- [34] J.E. Bertie, M.K. Ahmed, and H.E. Eysel, *J. Phys. Chem.* **93**, 2210 (1989).